Gamma

Physics Laboratory report

Group 28: Attilio Crognale and Javier Mariño Villadamigo

January 23, 2022

Contents

1 Introduction

On a daily basis, humans are exposed to different kinds of environmental radioactivity present in the soil, sea water, that produced by human action or present on Earth since its very creation. In this experience, a characterization of a NaI and a HPGe detector will be carried out (calibration and efficiency studies) so as to perform an analysis that will try to determine the magnitude of the environmental radioactivity of one of the most present elements in nature in the Veneto region: radon. Also, an analysis of different samples will be carried out to try to obtain the radioactive nuclides that compose them.

2 Experimental setup

The apparatus of the experiment consists of the following elements:

- A NaI detector used for high statistics measurements.
- A HPGe detector used for high precision energy measurements.
- A shielding container, made of a layer of lead and a layer of copper.
- A digitizer unit used to acquire and filter the signals.
- A sample of ^{60}Co, a sample of ^{241}Am and a sample of ^{152}Eu, all used for the characterization of the detectors.
- Various samples of different materials.
- A set of three canisters used for radon measurement.

3 Filter optimization

In this experiment it proved fundamental to distinguish between photopeaks coming from different gamma decays. To this regard, a filter was implemented in order to cut out part of noise.

Detector	FT	RT	Resolution(%)
NaI	80	300	5.19
HPGe	50	200	0.08

Table 1: Optimized parameters and relative resolutions.

The filter is represented by a trapezoidal distribution, which is convoluted with the output signal coming from the detectors. The filter is characterized by two main parameters, namely the flattop, FT, and the risetime, RT. The values of FT and RT were optimized in order to obtain the best possible resolution for the detectors, using the following procedure: the parameters of the trapezoid were set to default values. A spectrum of ^{60}Co was recorded for both detectors. The first peak of ^{60}Co was fit via a gaussian distribution and an estimate of the

efficiency was computed as (FWHM/centroid). The parameters of the trapezoid were then varied and new spectra were recorded. The efficiency was evaluated again for each detector and compared with the previous values.

This process was reiterated multiple times, in order to enhance the resolution of the detectors. The best results were obtained with the parameters shown in Table 1.

4 Characterization of the detectors

4.1 Calibration

Source	Peak (keV)	E (ch)	σ (ch)	Resolution (%)
		NaI		
^{241}Am	59	570.0(1)	26.6(1)	10.97(4)
^{60}Co	1173	9805(2)	199(2)	4.77(6)
^{60}Co	1333	11090(2)	218(3)	4.62(6)
		HPGe		
^{241}Am	59	340.0(2)	21.5(3)	14.9(2)
^{60}Co	1173	6727.7(1)	22.8(4)	0.80(1)
^{60}Co	1333	7642.6(1)	21.4(5)	0.66(2)

Table 2: Fitting results for the calibration of the three main energy peaks corresponding to the photons emitted by ^{241}Am and ^{60}Co.

The ^{60}Co sample was placed directly in front of the NaI detector, at a distance $d = 28.5(1)$ cm, and a spectrum was recorded. The ^{60}Co was then replaced with the ^{241}Am sample and a second spectrum was acquired. The three photopeaks present in the two spectra (two for ^{60}Co at 1172 keV and 1332 keV, and one for ^{241}Am at 59Kev) were fit to their own gaussian distributions. A conversion function was then obtained, allowing the passing from digitizers channels to energy along the rest of the experiment.

The samples of ^{60}Co and 241Am were moved in front of the HPGe, at a distance of $d = 20(1)$ cm. The calibration process was repeated for the HPGe detector. The results are summarized in Table 2.

Once the identification and fitting of the peaks position is done, what follows is a linear fit of their energy values with respect to their channel position. This is done in Fig. 2, with the respective fit results shown on the graphs.

4.2 Detection efficiency

The intrinsic efficiency of a detector can (and actually is) interpreted as the number of particles detected divided by the number of particles that reach the detector. Therefore, in order to know the intrinsic efficiency of a detector it is necessary to be in possession of the activity of the source at the time of measurement (i.e. know how many particles are going to be emitted during the acquisition time) and have a known geometric configuration (i.e. know how many of the emitted particles will actually enter the detector). The intrinsic efficiency of a detector can be therefore interpreted as the total efficiency (number of events registered divided by those emitted by the source) divided by the geometric acceptance (the solid angle that the detector subtends from the source):

$$\epsilon_i(E) = \frac{N_d(E)/N_e(E)}{\Delta\Omega/4\pi}, \tag{1}$$

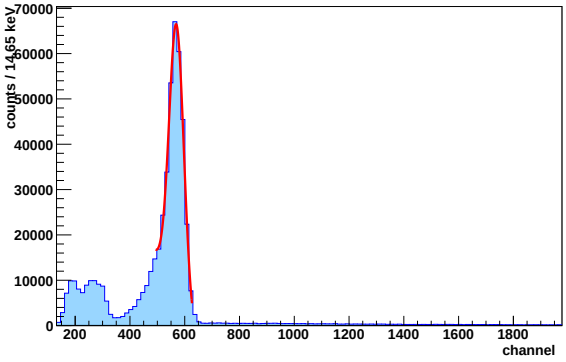

(a) Am peak in NaI scintillator.

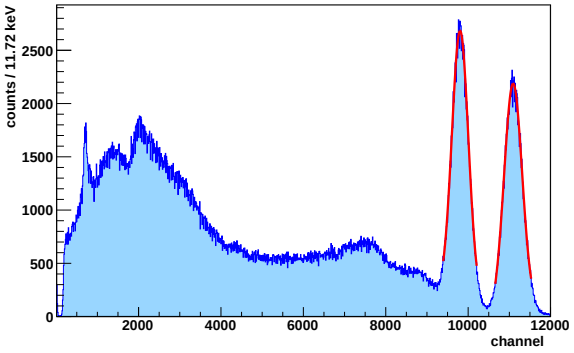

(b) Co peaks in NaI scintillator.

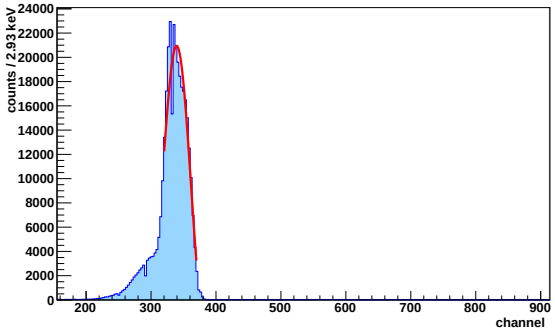

(c) Am peak in HPGe scintillator.

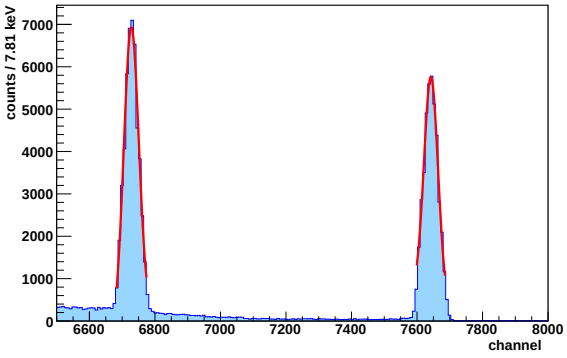

(d) Co peaks in HPGe scintillator.

Figure 1: Peak finding and fit of the three main peaks observed for both NaI (upper row) and HPGe (lower row) detectors.

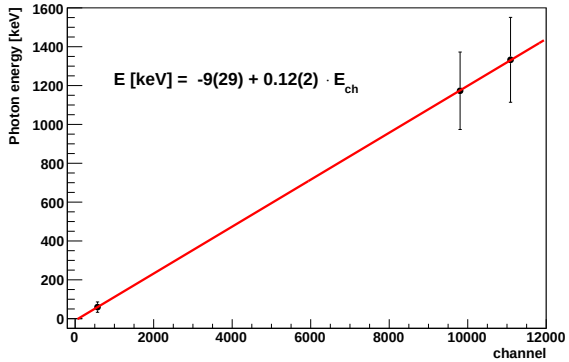

(a) Calibration fit for NaI detector.

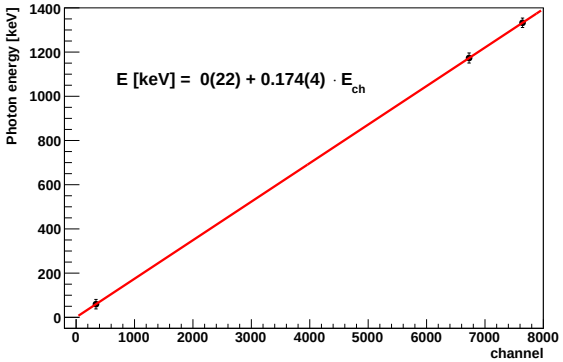

(b) Calibration fit for HPGe detector.

Figure 2: Calibration fits for both detectors. The results of the fit are shown on the graph, with considerably good χ^2 values.

where:

- $N_d(E)$ is the number of detected events in a certain energy peak. This is obtained from the integral of the peaks fit, once the background has been subtracted from the spectrum. An example of this is shown in Fig. 3, where the integral of each of the two ^{60}Co source is taken as $N_d(E)$.
- $N_e(E)$ is the number of photons emitted in a given photopeak and within a certain amount of time. This number is calculated based on the nominal activity of the source at the moment of measurement, the branching ratio of the peak of interest and the measurement time interval:

$$N_e(E) = A(E) \cdot BR(E) \cdot \Delta t. \tag{2}$$

- $\Delta\Omega$ is the solid angle subtended by the detector as seen from the source. This is calculated as $\Delta\Omega = \pi r^2/d^2$, where r is the radius of the detector, and d the distance between the latter and the source.

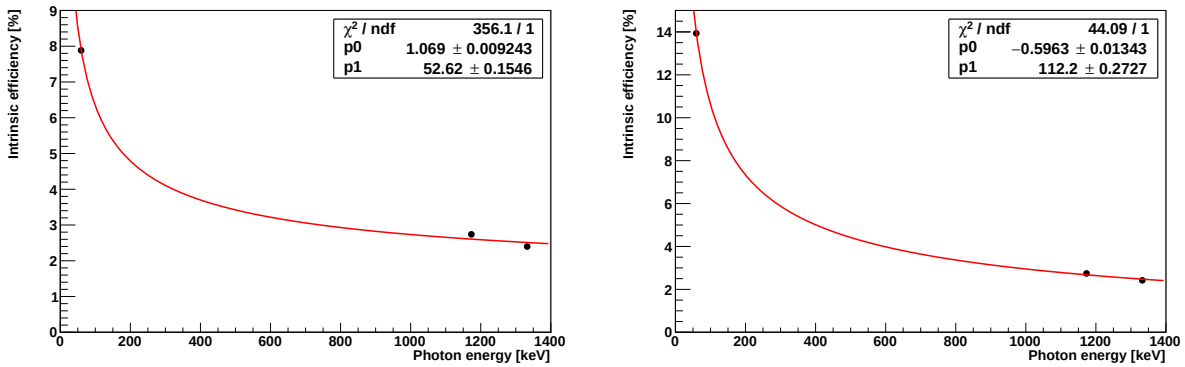

(a) Intrinsic efficiency fit for the three main peaks in NaI detector.

(b) Intrinsic efficiency fit for the three main peaks in HPGe detector.

Figure 4: Fit to Eq. 3 to obtain the intrinsic efficiency at any energy for both of the detectors.

Bearing this in mind, the process carried on was the computation of the intrinsic efficiency for each detector for the same three peaks used in calibration: those at 59, 1173 and 1333 keV, respectively. Therefore, making use of Eqs. 1 and 2, the intrinsic efficiency for each point is calculated and plotted in Fig. 4.

The data shown in Fig. 4 were fitted to the expression:

$$\epsilon_i = p_0 + p_1/\sqrt{E}, \tag{3}$$

which is demonstrated shows good agreement between resolutions (and therefore also efficiency) and energies.

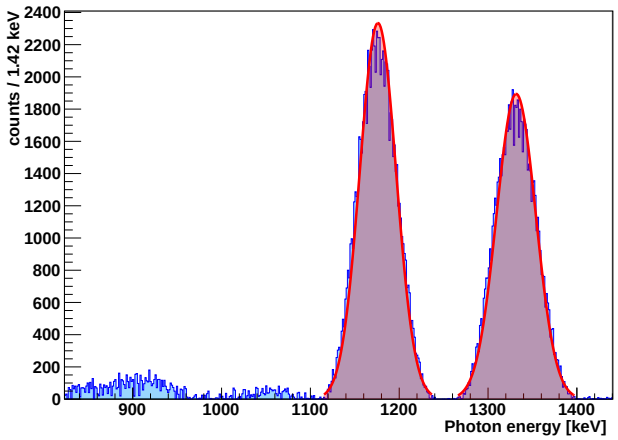

Figure 3: Visualization of the obtaining of $N_d(E)$ for each of the two ^{60}Co peaks and their corresponding integral in shaded area (performed in an interval $[\mu - 3\sigma, \mu + 3\sigma]$.

To be able to calculate these efficiencies, the distances between the source and NaI and HPGe detectors have been set to 28.5(1) cm and 20.0(1) cm, respectively. The geometric acceptance has been then calculated based on a point-like source and perfect alignment assumption, to finally yield the result $\Delta\Omega = \pi r^2/d^2$, to be introduced in Eq. 1, where r is the radius of the detector and d, the distance between the latter and the source. This is, however, a -fairly- poor approximation, but given the fact that the samples with which this analysis will be extended later are very diverse in shape, a detailed geometrical analysis is beyond the scope of this report.

In the case of NaI detector, the intrinsic efficiency will be obtained further on based on this fit, extrapolating its value from the parametrization given by Eq. 3 and the values obtained in Fig. 4(a). In the case of the HPGe, it is possible to perform a more precise study with the employment of a ^{152}Eu source. Selecting peaks of reasonably good quality (see Fig. 5), and knowing, a priori, the relative production yield between them, we are able to calculate a relative efficiency for these peaks, normalized to one of them. In this case, the standardized peak was that of 1408 keV. The selected peaks are shown in Table 3, where the integrals obtained, and their corresponding relative efficiency, are also shown.

In the case of the study of the relative efficiency for ^{152}Eu, a more precise fit can be put in action than that of Eq. 3. This time, a linear term can be added to improve the fit results at higher peak energies:

$$\epsilon_r = p_0 + p_1/\sqrt{E} + p_2/E.$$

The results of fitting this expression to the values shown in Table 3, are shown in Fig. 6 as the red line fitted to the black dots. The blue line is the fit performed to the intrinsic efficiency in Fig. 4(b). In order to use this fit to obtain the intrinsic efficiency of HPGe later on, the procedure to be carried out is a normalization of the red line to the blue line, at the point of reference previously used, i.e. 1408 keV. The result of this process is the green line in Fig. 6, which yields an interpolation as precise as possible for the calculation of the intrinsic detection efficiency at HPGe for a given photon energy.

5 Samples

The HPGe is a powerful tool in terms of detection resolution, as it can be seen from Table 2. Therefore, it can be used to analyze different samples from objects, and try to get, from their radioactive spectra, the elements that they are composed of. However, the HPGe detector does not have great efficiency, so a NaI detector analysis also is carried out to have more detection statistics.

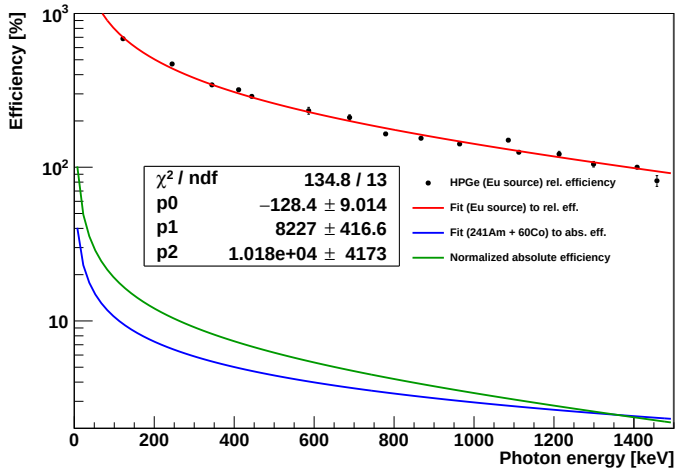

Figure 6: Relative efficiency study for ^{152}Eu peaks. In red, the fit for relative efficiency data; in blue, the calibration obtained in Fig. 4(b) and, in green, the normalization of the red curve to the blue one.

Peak (keV)	Integral	ϵ_r (%)
121.8	73700(200)	685(8)
344.3	33300(200)	343(4)
411.1	2600(50)	319(7)
444	3300(60)	289(6)
586.3	400(20)	233(12)
688.7	660(20)	211(9)
778.9	7860(90)	165(3)
867.4	2420(50)	154(4)
964	7610(90)	142(2)
1085.8	5570(70)	150(3)
1112.1	6200(80)	125(2)
1212.9	620(20)	122(5)
1299.1	620(20)	105(4)
1408	7630(90)	100(2)
1457.6	160(10)	82(7)

Table 3: ^{152}Eu chosen peaks (those marked in Fig. 5), to perform the relative efficiency analysis shown in Fig. 6.

To perform this analysis, the sample to be analyzed is put inside the shielding container, on top of the NaI detector (distance was estimated to be $d_{\mathrm{NaI}} = 2.5(1)$ cm). The distance from the HPGe detector was also measured to be $d_{\mathrm{HPGe}} = 7.5(1)$ cm. The activity related to one peak is then calculated as:

$$A = \frac{N_d}{\Delta\Omega/4\pi \cdot BR \cdot \Delta t},$$

where $\Delta\Omega$ is the solid angle subtended by the detector, N_d is the number of events recorded in a certain photopeak, BR is the branching ratio for the dicussed decay and Δt is the amount of acquisition time. In order to have a measure of the activity per unit of mass, the activity is also divided by the mass of the sample, then having $A_m \equiv A/m$.

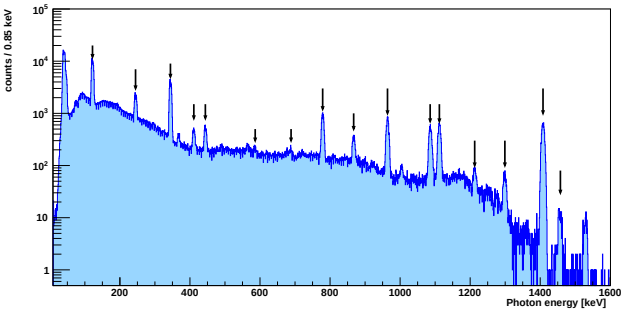

Figure 5: Selection of the Eu peaks valid for relative efficiency studying.

5.1 KCl

The first object to be analyzed was a sample of 8 g of KCl. A spectrum of 15 minutes was acquired, and also a 29 minutes background spectrum. The background spectrum was subtracted to the KCl one

with a proper time normalization factor, although in the following analysis is not shown, for simplicity. The acquired spectra in NaI and HPGe only seemed to show one relevant peak, at ~ 1460 keV.

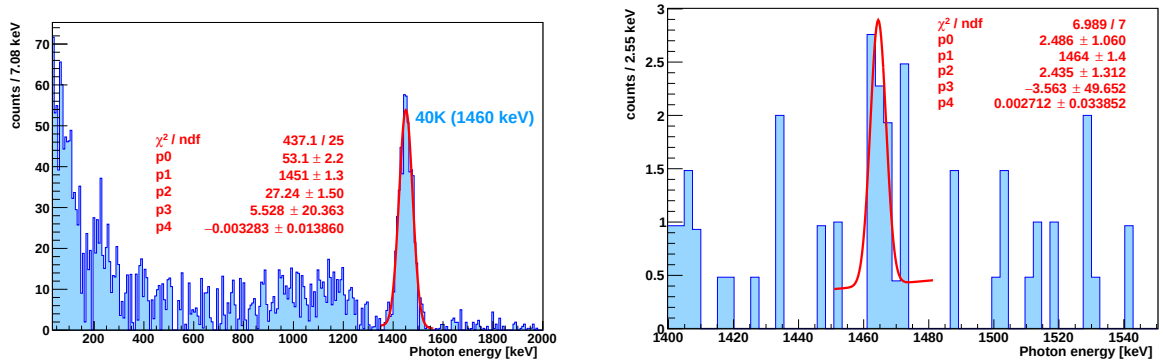

(a) KCl in NaI.

(b) KCl in HPGe.

Figure 7: KCl spectra.

Therefore, the total activity of the sample is only the one due to 1461 keV peak. The results shown in Table 4 differ, however, significantly from those written in the lab guide, that is, 12 Bq of total activity in the sample of 8 g, therefore $A_m^{\text{theo}} \approx 1.5$ Bq/g. This result is evidently wrong and there are various reasons due to which it can be. First, the result obtained from HPGe is very imprecise, given the fact that the acquired statistics are extremely low and therefore great variations would not be unexpected. On the other hand, the NaI detector geometric configuration is not optimal: although the advised position to situate the source was right on top of the NaI detector, this complicates greatly the labor of obtaining a proper geometrical window, since a point-like source is no good approximation. The intrinsic efficiency could therefore have been biased since the first calculation and a simple model like the one used here will hardly yield reliable results.

Peak (keV)	Nuclide	E_γ (keV)	σ (keV)	N_d	BR	A_m (Bq/g)
			NaI			
1461	^{40}K	1451(1)	27(2)	530(2)	0.1067	48.251
			HPGe			
1461	^{40}K	1464(1)	2(1)	35(6)	0.1067	104.979

Table 4: Results obtained for the only peak found in KCl sample.

5.2 Pellets ashes

The second sample used was the ashes of 250 g of burned pellets. Surprisingly, the results of the spectra inspection brought the appearance of numerous peaks of the $4n$ decay chain (also named thorium chain) and some also from the $4n + 2$ chain (or uranium chain). The spectra obtained (already with the subtracted background) are shown in Fig. 8. A fit to each peak is also done to obtain the mean energy value of the decay gamma, and the integral of the peak, above other data. Finally, the activity per unit of gram for each peak is displayed in the last column of Table 5. As it can be seen from Table 5, four out of seven of the most relevant peaks found, correspond to the uranium decay chain, which suggests that the pellets were highly exposed to this element in the previous years.

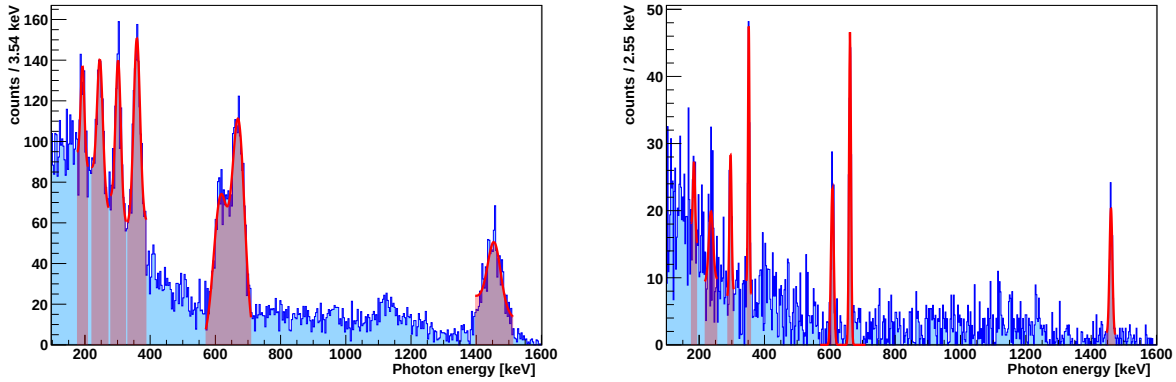

(a) Pellets in NaI.

(b) Pellets in HPGe

Figure 8: Pellets spectra.

Peak (keV)	Nuclide	E_γ (keV)	σ (keV)	N_d	BR	A_m (Bq/g)
				NaI		
186	^{226}Ra ($4n+2$ chain)	193(1)	6(1)	1090(30)	0.055	3.041
239	^{212}Pb ($4n$ chain)	246(1)	8(1)	1470(40)	0.44	0.565
295	^{214}Pb ($4n+2$ chain)	302.2(9)	9(1)	1400(40)	0.18	1.418
352	^{214}Pb ($4n+2$ chain)	359.6(9)	9(1)	1580(40)	0.36	0.853
609	^{214}Po ($4n+2$ chain)	616(2)	21(2)	1060(30)	0.449	0.556
662	^{137}Cs	670(1)	19(1)	1440(40)	0.946	0.369
1461	^{40}K	1454(3)	23(5)	1050(30)	0.1067	3.048
				HPGe		
186	^{226}Ra ($4n+2$ chain)	184(2)	3(2)	160(10)	0.055	0.140
239	^{212}Pb ($4n$ chain)	236(5)	6(4)	210(10)	0.44	0.028
295	^{214}Pb ($4n+2$ chain)	296.1(5)	3.3(4)	130(10)	0.18	0.048
352	^{214}Pb ($4n+2$ chain)	351.9(1)	2.4(2)	140(10)	0.36	0.029
609	^{214}Po ($4n+2$ chain)	607.9(6)	4.3(6)	100(10)	0.449	0.026
662	^{137}Cs	661.9(3)	3.1(2)	140(10)	0.946	0.019
1461	^{40}K	1460.7(5)	4.4(6)	100(9)	0.1067	0.254

Table 5: Data obtained from the peak search in pellets sample.

It is interesting to note, also, a contribution of ^{137}Cs (which is mainly human-produced) that nearly overlaps with the peak of ^{214}Po (see Fig. 8(a)). The importance of HPGe comes now into play, when it shows that these two peaks are indeed two distinct ones in Fig. 8(b). The total activity of the sample can now be obtained as $A_m = \sum_{\text{peaks}} A_{m,\,i}$. Then using the data from Table 5, one obtains:

$$A_m^{\text{NaI}} = 9.85 \text{ Bq/g}, \qquad A_m^{\text{HPGe}} = 0.544 \text{ Bq/g}.$$

Naturally, these two should be equivalent, but the problems already commented in the case of the KCl sample are not negligible in this case either. This time, however, the statistics of HPGe detector are

considerably better and, given the fact that its geometric configuration is, as stated, a more suitable situation to use point-like approximation than that of NaI, it might be expected that the *actual* activity per unit of mass of the pellets sample is closer to A_m^{HPGe} than to A_m^{NaI}.

6 Radon

6.1 Environmental radon

The measurement of environmental radon activity was done following EPA standard procedure. As stated previously, three canisters were used in this part of the experiment: a canister that was not exposed to the environment, named **background**; a canister with a fixed amount of radon activity, named **reference** and a third canister, named **exposed**.

The **exposed** canister was weighted, and then left open in the room of the measurement of Polo Didattico. After two days the **exposed** canister was retrieved, sealed, and weighted again. The difference in mass Δm before and after the exposure corresponds to the mass of water vapor absorbed during the exposure, also referred to as "water gain". In short:

$$\Delta m = \text{water gain [g]} = 2.6(0.1)\ \text{g}.$$

Knowing the value of Δm, it is possible to obtain the value of the calibration factor, CF. In this case, $CF = 0.16(1)\ \text{l} \cdot \text{min}^{-1}$.

The **background** canister was placed inside the shielding container and a background run was recorded. The **background** canister was replaced with the **reference** canister, and a spectrum was acquired for each detector.

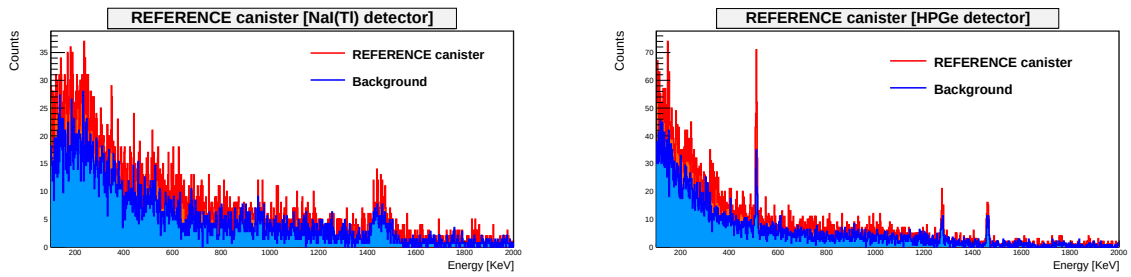

(a) NaI detector.

(b) HPGe detector.

Figure 9: Spectra obtained from the **reference** canister.

The spectra in Fig. 9 were studied in order to obtain E, defined as the total number of events in the gamma peaks divided by the activity of the **reference** canister. The results are shown below.

$$E_{\text{NaI}} = 9,56(4)\ \text{pCi}^{-1}, \qquad E_{\text{HPGe}} = 0.104(1)\ \text{pCi}^{-1}$$

The **reference** canister was removed, and the **exposed** canister was placed inside the shielding container. A spectrum was recorded for each detector.

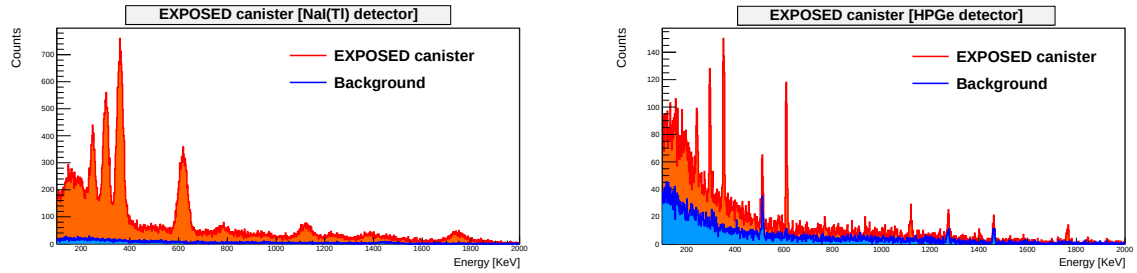

(a) NaI detector.

(b) HPGe detector.

Figure 10: Spectra obtained from **exposed** canister.

From the analysis of the spectra in Fig. 10 it was possible to calculate N, defined as the sum of events present in all gamma peaks (once the background is removed). The results obtained for the two detectors read as follows:

$$N_{\text{NaI}} = 967800(900), \qquad N_{\text{HPGe}} = 25800(160).$$

In order the evaluate the radon activity, it is also important to take into account the fact some radon in the **exposed** canister decayed before the measurement. This effect is expressed via a decay factor DF, defined as

$$DF = \exp(-0.693 \cdot t/T_{1/2}),$$

where t is the difference between the time at half exposure and the time of measurement, while $T_{1/2}$ is the half-life of radon. In this case $t = 1475(1)$ min yielding $DF = 0.8304(2)$.

Once all necessary quantities are determined, it is possible to evaluate the radon activity per liter of air as

$$RN = \frac{N}{E \cdot CF \cdot DF \cdot T_{\text{exp}}}$$

where $T_{\text{exp}} = 2910(1)$ min is the time of exposure. The final result yields

$$RN_{\text{NaI}} = 2030(70)\ \text{pCi} \cdot \text{L}^{-1} = 75(3)\text{Bq} \cdot \text{L}^{-1}, \quad RN_{\text{HPGe}} = 1280(30)\text{pCi} \cdot \text{L}^{-1} = 47(1)\text{Bq} \cdot \text{L}^{-1}.$$

The two detectors yield different values, as for previous activity measurements. However the estimates obtained are still of the same order of magnitude.

6.2 Autunite

Once completed the measurement of environmental radon, the canister was replaced by a sample of autunite, a strongly active material containing uranium. The measuring procedure is the same used for previous samples

From the spectra in Fig. 11 it was possible to estimate the activity of the sample.

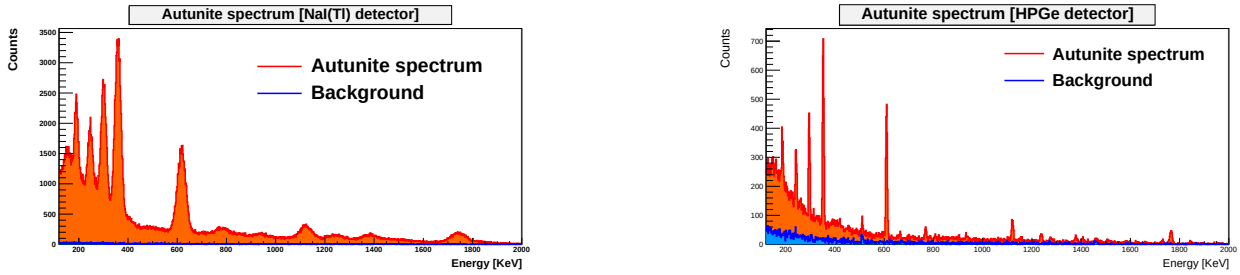

(a) NaI detector.

(b) HPGe detector.

Figure 11: Spectra obtained from autunite sample.

Peak (keV)	Nuclide	E_γ (keV)	σ (keV)	N_d	BR	A_m (Bq/g)
			NaI			
186	^{226}Ra ($4n+2$ chain)	190(1)	8(3)	9547(90)	0.055	227
239	^{212}Pb ($4n$ chain)	246(3)	9(3)	11000(100)	0.44	36
295	^{214}Pb ($4n+2$ chain)	300(5)	9(6)	24300(100)	0.18	211
352	^{214}Pb ($4n+2$ chain)	359(2)	11(5)	44600(200)	0.36	206
609	^{214}Po ($4n+2$ chain)	617(1)	19(3)	29100(200)	0.449	130
1120	^{214}Bi	1122(2)	21(2)	5680(70)	0.15	91
			HPGe			
186	^{226}Ra ($4n+2$ chain)	186(2)	2(2)	700(30)	0.055	119
239	^{212}Pb ($4n$ chain)	242(2)	3(1)	671(20)	0.44	17
295	^{214}Pb ($4n+2$ chain)	295.2(6)	2.6(9)	1320(50)	0.18	95
352	^{214}Pb ($4n+2$ chain)	352.0(3)	2.7(3)	2350(50)	0.36	96
609	^{214}Po ($4n+2$ chain)	609.4(1)	3.1(5)	1790(40)	0.449	89
1120	^{214}Bi	1120.3(3)	3.5(7)	360(20)	0.15	93

Table 6: Data obtained from the peak search in autunite sample.

7 Conclusions

Using the samples of known activity, provided by the laboratory, it was possible to obtain the intrinsic efficiency for both detectors. In the case of HPGe it was also possible to obtain a relative efficiency curve using the sample of ^{152}Eu. The activity of various samples was successfully measured, and it was possible to identify the nuclides responsible for the gamma peaks present in the spectra. The values of the activities varied significantly based on the detector, but the imprecision of the approximations taken could have played a significant role in that variation. It was possible to measure the radon activity in the environment, and obtain two different estimate for the two detectors. In the case of autunite, as for the other samples, the activity was successfully measured.